

---

# Two class I very low-mass objects in Taurus

---

C. Dang-Duc<sup>1,2</sup> and N. Phan-Bao<sup>1</sup>

CUONGPHYSICS3@GMAIL.COM

<sup>1</sup>*Department of Physics, HCM International University-VNU, Block 6, Linh Trung Ward, Thu Duc District, HCM city, Viet Nam.*

<sup>2</sup>*Faculty of Physics and Engineering Physics, HCM University of Science-VNU, 227 Nguyen Van Cu Street, District 5, HCM city, Viet Nam.*

## Abstract

We report our study of two proto-brown dwarf candidates in Taurus, [GKH94] 41 and IRAS 04191+1523B. Based on continuum maps at 102 GHz (or 2.9 mm), spectral types and the spectral energy distribution of both targets, we confirmed the class I evolutionary stage of [GKH94] 41 and IRAS 04191+1523B, and estimated the upper limit to the final masses to be  $49_{-27}^{+56} M_J$  and  $75_{-26}^{+40} M_J$  for [GKH94] 41 and IRAS 04191+1523B, respectively. This indicates that they will likely end up as brown dwarfs or very low-mass stars. The existence of these class I very low-mass objects strongly supports the scenario that brown dwarfs and very low-mass stars have the same formation stages as low-mass stars.

## 1. Introduction

Up to date, many class II brown dwarfs (BDs) have been discovered in different star-forming regions. Observations of statistical properties of these class II BDs have strongly supported the scenario that BDs form like low-mass stars (see Luhman 2012 and references therein). However, it remains unclear how the BD formation process occurs at the earliest evolutionary stages such as BD core, class 0 and class I, which contain key pieces to fully understand the BD formation mechanism. So far, a few class 0/I proto-BD candidates have been identified (e.g., Bourke et al. 2006; Lee et al. 2013; Palau et al. 2014; Morata et al. 2015; Liu et al. 2016) but only two objects of them, L328-IRS (Lee et al. 2013) and IC 348-SMM2E (Palau et al. 2014), have been classified as class 0 BDs with estimated final masses below the substellar boundary. The first pre-BD core that has been identified so far is Oph B-11 in rho Ophiuchi (André et al. 2012).

In this paper, we present our identification of two confirmed class I very low-mass (VLM) objects in Taurus, [GKH94] 41 and IRAS 04191+1523B.

## 2. Sample and observational data

We selected two class I proto-BD candidates, [GKH94] 41 and IRAS 04191+1523B, in the list of 352 members of Taurus published in Luhman et al. 2010.

[GKH94] 41 has an estimated spectral type of  $M7.5 \pm 1.5$  (Luhman et al. 2009). The source was classified as a class I or very young class II object. Furlan et al. 2011 then classified [GKH94] 41 as a class II object because its dereddened SED is similar to the SED of a typical T Tauri star.

IRAS 04191+1523B is the secondary component of a 6.1'' binary (Duchêne et al. 2004). The source has a spectral type of M6–M8 (Luhman et al. 2010). In this paper, we adopted a spectral type of  $M7.0 \pm 1.0$  for the object. IRAS 04191+1523B was classified as a class I object in Luhman et al. 2010.

Observational data at infrared, submm and mm wavelengths of the targets available in the literature are listed in Table 1.

We searched for millimeter continuum observations of two targets in the Combined Array for Research in Millimeter-wave Astronomy (CARMA) data archive. [GKH94] 41 and IRAS 04191+1523B were observed on 2012 December 25 at 102 GHz frequency (or 2.9 mm wavelength). We then reduced the continuum data using the MIRIAD package adapted for CARMA.

## 3. Results and discussion

The continuum maps of [GKH94] 41 and IRAS 04191+1523B are shown in Figure 1. Using the Gaussian fitting, we measured the integrated fluxes of [GKH94] 41, IRAS 04191+1523A and IRAS 04191+1523B to be  $2.5 \pm 0.2$  mJy,  $9.5 \pm 0.4$  mJy and  $5.6 \pm 0.4$  mJy (see Table 2), respectively. The deconvolved sizes of the continuum emission from [GKH94] 41 and IRAS 04191+1523A are listed in Table 2. For the case of IRAS 04191+1523B, the 2D Gaussian fitting was not able to deconvolve the emission, which appears to be a point source with the current spatial resolution.

Table 1. Photometry for [GKH94] 41 and IRAS 04191+1523AB

Two class I very low-mass objects in Taurus				
Source	Wavelength ( $\mu\text{m}$ )	Flux (mJy)	Error (mJy)	References
[GKH94] 41	1.65	2.5	0.1	(Cutri et al. 2003)
	2.17	11.7	0.3	(Cutri et al. 2003)
	3.4	15	0.4	(Wright et al. 2010)
	3.6	27.3	0.5	(Luhman et al. 2010)
	4.5	34.2	0.7	(Luhman et al. 2010)
	4.6	30.9	0.7	(Wright et al. 2010)
	5.8	41.8	0.9	(Luhman et al. 2010)
	8	37.5	0.9	(Luhman et al. 2010)
	12	46	1	(Wright et al. 2010)
	22	196	5	(Wright et al. 2010)
	24	172	10	(Harvey et al. 2012)
	70	269	5	(Bulger et al. 2014)
	160	279	66	(Bulger et al. 2014)
IRAS 04191+1523AB	2940	2.5	0.2	(Dang-Duc, Phan-Bao, & Dao-Van 2016)
	70	7002	13	(Bulger et al. 2014)
	160	8884	232	(Bulger et al. 2014)
	450	3940	220	(Francesco et al. 2008)
	850	1380	20	(Francesco et al. 2008)
	1300	110	7	(Motte & André 2001)
	2940	9.5 <sup>a</sup>	0.4 <sup>a</sup>	(Dang-Duc, Phan-Bao, & Dao-Van 2016)
		5.6 <sup>b</sup>	0.4 <sup>b</sup>	(Dang-Duc, Phan-Bao, & Dao-Van 2016)

**Note:**

<sup>a</sup>: the flux and its error for IRAS 04191+1523A.

<sup>b</sup>: the flux and its error for IRAS 04191+1523B.

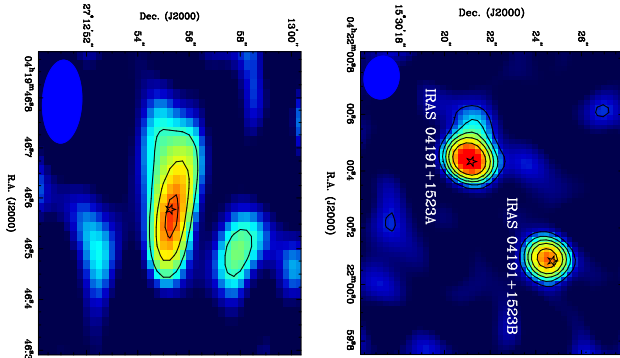


Figure 1. **Left panel:** Continuum map at 102 GHz of [GKH94] 41. The star symbol shows the 2MASS near-infrared position of [GKH94] 41. The contours are -3, 3, 5 and 7 times the rms of 0.2 mJy beam<sup>-1</sup>. The synthesized beam is shown in the bottom left corner. **Right panel:** Continuum map at 102 GHz of IRAS 04191+1523A and IRAS 04191+1523B. The star symbols show the 2MASS near-infrared positions of the components. The contours are -3, 3, 5, 7, 9 and 12 times the rms of 0.4 mJy beam<sup>-1</sup>. The synthesized beam is shown in the bottom left corner.

**3.1. Determination of the evolutionary stages of [GKH94] 41 and IRAS 04191+1523B**

For the case of [GKH94] 41, the deconvolved major axis of the emission from the source is about 2.9'' (see Table 2) or about 400 AU in length at a distance of 140 pc of Taurus. This size of the emission is considerably larger than the typical size of disks around class II BDs (140–280 AU, e.g., Ricci et al. 2014). This suggests that the compact structure associated with the source is dominated by an envelope. [GKH94] 41 is therefore a class I object. Using the observational data in Table 1, we also estimated the bolometric temperature of [GKH94] 41 to be  $\sim 460$  K. This value indicates that the source is in the late class I evolutionary stage (300–650 K, Enoch et al. 2009).

For IRAS 04191+1523B, it was classified as a class I object in Luhman et al. 2010. Our continuum map (see Figure 1) spatially resolves the binary into two components with a separation of 6.1'', which is consistent with the previous value as reported in Duchêne et al. 2004. Both components are associated with envelopes. This therefore confirms the Luhman et al. classification of the source.

Table 2. Parameters of the continuum regions around GKH94] 41, IRAS 04191+1523A, and IRAS 04191+1523B

Source	Deconvolved major axis (")	Deconvolved minor axis (")	Flux (mJy)
[GKH94] 41	$2.9 \pm 0.1$	$0.3 \pm 0.1$	$2.5 \pm 0.2$
IRAS 04191+1523A	$1.4 \pm 0.1$	$0.3 \pm 0.1$	$9.5 \pm 0.4$
IRAS 04191+1523B	$1.8 \pm 0.1^a$	$1.6 \pm 0.1^a$	$5.6 \pm 0.4$

**Note:** <sup>a</sup>: Undeconvolved values.

### 3.2. Estimate of the final masses of [GKH94] 41 and IRAS 04191+1523B

To determine the substellar nature of [GKH94] 41 and IRAS 04191+1523B, we estimate the upper limit to the final masses of these objects. Since the accretion mass that is added to the central object should be lower than the mass of the envelope associated with the object. Therefore, the upper limit to the final mass of a stellar object can be determined from the current mass of the central object and the mass of its envelope.

#### 3.2.1. [GKH94] 41: A CLASS I BD

Assuming an age of 1 Myr for [GKH94] 41 and using the effective temperature versus mass relation of the DUSTY model (Chabrier et al. 2000), we estimated the current mass of [GKH94] 41. A spectral type of M7.5 gives its effective temperature of about 2795 K (Luhman et al. 2003). According to the DUSTY model, this temperature value corresponds to a mass of  $41 M_J$ . If the uncertainty of 1.5 subclasses in the spectral type is taken into account, then the mass of the object is in the range of 14–97  $M_J$ .

To estimate the envelope mass of [GKH94] 41, we searched for the best fit of a modified blackbody to the SED of the source with fluxes from 70  $\mu\text{m}$  to mm wavelengths (Table 1) as done for IC348-SMM2E (see Palau et al. 2014). The best fit (Figure 2) gives dust temperature  $T_d = 34$  K, dust emissivity  $\beta = 0.4$ , and envelope mass  $M_{\text{env}} = 2 M_J$ . Our estimated dust emissivity is considerably smaller than the typical value of 1.4 for class I objects in Taurus (Chandler et al. 1998). The discrepancy is probably due to our best fit obtained with only three data points available for the source. If we use  $\beta = 1.4$  and  $T_d = 34$  K to estimate the envelope mass of [GKH94] 41 directly from the flux at 2.9 mm, we obtain an envelope mass of 8  $M_J$ . We then adopted an envelope mass of 8  $M_J$  for [GKH94] 41.

With the current mass of 41  $M_J$  and the envelope mass of 8  $M_J$ , the upper limit to the final mass of [GKH94] 41 is therefore 49  $M_J$ . If we include the spec-

tral type uncertainty of the central object, the upper limit is  $49_{-27}^{+56} M_J$ . This indicates that [GKH94] 41 will very likely end up with a substellar mass.

#### 3.2.2. IRAS 04191+1523B: A CLASS I VLM OBJECT

The final mass of IRAS 04191+1523B was also estimated using the same steps as done for [GKH94] 41. A spectral type of M7.5 of IRAS 04191+1523B gives an effective temperature of about 2880 K. Based on the DUSTY model, this temperature value corresponds to a mass of 57  $M_J$ . If we include the uncertainty of 1.0 subclass in its spectral type, a possible mass range for the object will be 31–97  $M_J$ .

Because the fluxes at infrared and submm wavelengths (from 70  $\mu\text{m}$  to 1.3 mm) are unresolved for components A and B (Table 1). We therefore estimated the total mass of the envelopes associated with the two components. We then obtained the best fit for IRAS 04191+1523AB (Figure 2) with  $T_d = 32$  K,  $\beta = 0.7$ , and  $M_{\text{env}} = 33 M_J$ . Since the fluxes at 2.9 mm were resolved for components A and B. Therefore, the envelope mass of each component could be estimated directly from the 2.9 mm fluxes. If we use  $\beta = 1.4$  (Chandler et al. 1998) and  $T_d = 32$  K, we obtain envelope masses of 31  $M_J$  for IRAS 04191+1523A and 18  $M_J$  for IRAS 04191+1523B, respectively. We then adopted an envelope mass of 18  $M_J$  for component B.

With the current mass of 57  $M_J$  and the envelope mass of 18  $M_J$ , the upper limit to the final mass of IRAS 04191+1523B is 75  $M_J$ . If the uncertainty in its spectral type is taken into account, the upper limit is  $75_{-26}^{+40} M_J$ . This suggests that IRAS 04191+1523B will end up as a BD or VLM star.

## 4. Conclusion

We report here our study of two class I BD candidates in Taurus, [GKH94] 41 and IRAS 04191+1523B. Our mass estimates indicate that they will end up as BDs or VLM stars. The existence of these class I VLM objects

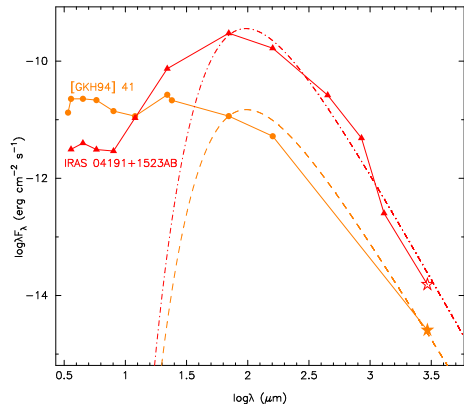


Figure 2. SEDs of [GKH94] 41 (brown line) and IRAS 04191+1523AB (red line). The solid and open star symbols show the fluxes at 2.9 mm (or 102 GHz) of [GKH94] 41 and IRAS 04191+1523AB, respectively. The best fit for a modified blackbody of the dust envelope of [GKH94] 41 (brown dashed-line) and IRAS 04191+1523AB (red dash-dotted line) is also shown.

together with two class 0 BDs and one pre-BD core as previously reported in the literature has demonstrated that BDs and low-mass stars have similar evolutionary tracks.

## Acknowledgments

This research is funded by Vietnam National Foundation for Science and Technology Development (NAFOSTED) under grant number 103.99-2015.108. C.D.-D. gratefully acknowledges financial support from the Local Organizing Committee of the Star Formation in Different Environments Conference held in ICISE, Quy Nhon, Vietnam on July 25-29th, 2016. Support for CARMA construction was derived from the Gordon and Betty Moore Foundation, the Kenneth T. and Eileen L. Norris Foundation, the James S. McDonnell Foundation, the Associates of the California Institute of Technology, the University of Chicago, the states of California, Illinois, and Maryland, and the National Science Foundation. Ongoing CARMA development and operations are supported by the National Science Foundation under a cooperative agreement, and by the CARMA partner universities.

## References

Chandler, C. J., Barsony, M., & Moore, T. J. T. 1998, MNRAS, 299, 789  
 Luhman, K. L., et al. 2003, ApJ, 593, 1093  
 Chabrier, G., et al. 2000, ApJ, 542, 464

Enoch, M. L., et al. 2009, ApJ, 692, 973  
 Ricci, L., et al. 2014, ApJ, 791, 20  
 Motte, F., & André, P. 2001, A&A, 365, 440  
 Francesco, J. D., et al. 2008, ApJS, 175, 277  
 Dang-Duc, C., Phan-Bao, N., & Dao-Van, D.T. 2016, A&A, 588, L2  
 Bulger, J., et al. 2014, A&A, 570, A29  
 Harvey, P. M., et al. 2012, ApJ, 755, 67  
 Wright, E. L., et al. 2010, AJ, 140, 1868  
 Cutri, R. M., et al. 2003, VizieR Online Data Catalog: II/246  
 Duchêne, G., et al. 2004, A&A, 427, 651  
 Furlan, E., et al. 2011, ApJS, 195, 3  
 Luhman, K. L., et al. 2009, ApJ, 703, 399  
 Luhman, K. L., et al. 2010, ApJS, 186, 111  
 André, P., Ward-Thompson, D., & Greaves, J. 2012, Science, 337, 69  
 Liu, T., et al. 2016, ApJS, 222, 7  
 Morata, O., et al. 2015, ApJ, 807, 55  
 Palau, A., et al. 2014, MNRAS, 444, 833  
 Lee, C. W., et al. 2013, ApJ, 777, 50  
 Bourke, T. L., et al. 2006, ApJ, 649, L37  
 Luhman, K. L. 2012, ARA&A, 50, 65